Published in final edited form as:
J Alzheimers Dis. 2013 January 1; 33(1): 249–263. doi:10.3233/JAD-2012-121093.

Characteristics of TBS-extractable hyperphosphorylated tau species: Aggregation intermediates in rTg4510 mouse brain

Naruhiko Sahara[1,2], **Michael DeTure**[2], **Yan Ren**[1], **Abdul-Shukkur Ebrahim**[2,*], **Dongcheul Kang**[2], **Joshua Knight**[1,2], **Christiane Volbracht**[3], **Jan Torleif Pedersen**[3], **Dennis W. Dickson**[2], **Shu-Hui Yen**[2], and **Jada Lewis**[1,2]

[1]Center for Translational Research in Neurodegenerative Disease and Department of Neuroscience, University of Florida, 1275 Center Drive, Gainesville, FL 32610, USA

[2]Department of Neuroscience, Mayo Clinic, 4500 San Pablo Road, Jacksonville, Florida 32224, USA

[3]H. Lundbeck A/S, Copenhagen, Denmark

Abstract

Conditional overexpression of four-repeat human tau containing the P301L missense mutation in the rTg4510 mouse model of tauopathy leads to progressive accumulation of neurofibrillary tangles and hyperphosphorylated, sarkosyl-insoluble tau species, which are biochemically comparable to abnormal tau characteristic of hereditary tauopathies termed FTDP-17. To fully understand the impact of tau species at different stages of self-assembly on neurodegeneration, we fractionated rTg4510 brain representing several stages of tauopathy to obtain TBS-extractable (S1), high salt/sarkosyl-extractable (S3), and sarkosyl-insoluble (P3) fractions. Under reducing condition, the S1 fraction was demonstrated by Western blotting to contain both 50–60 kDa normally-sized and 64 kDa tau. Both are thermo-stable, but the 64 kDa tau showed a higher degree of phosphorylation. Under non-reducing condition, nearly all TBS-extractable 64 kDa tau were detected as ~130 kDa species consistent with the size of dimer. Quantitative analysis showed ~80 times more 64 kDa tau in S1 than P3 fraction. Immunoelectron microscopy revealed tau-positive granules/short filaments in S1 fraction. These structures displayed MC1 immunoreactivities indicative of conformational/pathological change of tau. MC1 immunoreactivity was detected by dot blotting in samples from 2.5 month-old mice, whereas Ab39 immunoreactivity indicative of late stages of tau assembly was detected only in P3 fraction. Quantitative analysis also demonstrated a significant inverse correlation between brain weight and 64 kDa tau, but the level of TBS-extractable 64 kDa tau reflects neurodegeneration better than that of sarkosyl-insoluble 64 kDa tau. Together, the findings suggest that TBS-extractable 64 kDa tau production is a potential target for therapeutic intervention of tauopathies.

Keywords

tau protein; tauopathy; transgenic mice; FTDP-17; hyperphosphorylation; dimer

Corresponding author: Naruhiko Sahara, Department of Neuroscience, Center for Translational Research in Neurodegenerative Disease, University of Florida, 1275 Center Drive, Gainesville, FL 32610, USA, Phone: +1-352-273-9661, Fax: +1-352-294-5060, nsahara@ufl.edu.
*Current address: Department of Internal Medicine, Wayne State University, 540E Canfield, Detroit, MI 48202

INTRODUCTION

Accumulation of intracellular neurofibrillary tangles (NFTs) consisting of microtubule-associated protein tau is a major hallmark of Alzheimer's disease (AD) and related diseases regarded as tauopathies [1–3]. Tau protein derived from NFTs is insoluble in the detergent sarkosyl and has elevated levels of both phosphorylation and ubiquitination - features that distinguish NFTs from normal tau protein. In human tauopathies, accumulation of fibrillary tau and neuronal loss have been localized in brain regions associated with cognitive dysfunction [4], suggesting a close link between these features. This notion is supported by studies of transgenic animals overexpressing human tau (hTau) [5–12]. The rTg4510 mouse model expresses mutant hTau containing the frontotemporal dementia with parkinsonism linked to tau on chromosome 17 (FTDP-17-Tau) associated P301L mutation and hTau expression can be by suppressed doxycycline [13,14]. In rTg4510 mice, expression of P301L hTau induces NFT formation, neuronal loss and behavioral abnormalities (e.g. memory dysfunction) in an age-dependent manner. Importantly, changes in memory index have been noted in rTg4510 prior to the appearance of sarkosyl-insoluble tau, suggesting a poor relationship between sarkosyl-insoluble tau production and memory impairment [15]. Furthermore, suppression of hTau halted neuronal loss and partially reversed cognitive dysfunction without preventing NFTs [14], suggesting that NFTs themselves are not initially cytotoxic. Thus, the initial mechanisms that lead to neuronal death and memory impairment in these mice remain unclear.

Studies of brain specimens from individuals with AD indicate that the progression of tauopathy is likely to involve different pools of tau [16]. A pool of hyperphosphorylated tau —referred to as AD-P tau— previously has been isolated from AD brains through differential centrifugation [16]. This form of tau was recovered from a pellet fraction (27,000 × g to 200,000 × g) from AD brains homogenized in a buffer containing 0.32 M sucrose [16]. AD-P tau does not appear to associate with any filamentous elements, yet it is able to self-assemble into filaments comparable to those that accumulate in AD brains [17]. Furthermore, two additional pools of hyperphosphorylated abnormal tau have been identified based on their solubility in sarkosyl [18].

Due to the rapid progression of tau pathology in specific brain regions and the conditional expression of tau, the rTg4510 mouse model has proven to be a useful tool for investigating the progression of tauopathy. These mice produce 140 and 170 kDa abnormal tau species, the level of which is significantly and negatively correlated to the memory index of the mice [15]. The 140 kDa tau and normal tau are similar in solubility, and both can be recovered in the supernatant fraction obtained by centrifuging brain extracts at 150,000 × g for 15 min. In comparison, the 170 kDa species is primarily sarkosyl-insoluble. Both 140 and 170 kDa tau represent a very small proportion of total tau in rTg4510 mice; however, they have been considered as tau species at early-stages of aggregation [15]. Regardless, it remains unclear as to changes of different tau pools during the progression of tauopathy. To address these issues, we examined the profile and solubility of tau protein using specimens derived from 2 to 14 month-old rTg4510 mice and characterized a pool of TBS-extractable tau in depth.

EXPERIMENTAL PROCEDURES

Mice

The parental mutant hTau responder line, parental tTAactivator line, and the resultant F1 rTg4510 mice and littermates were generated and maintained as previously described by SantaCruz et al. [14]. Mice were maintained on a standard diet lacking doxycycline to ensure that transgenic hTau was expressed throughout the lifetime of the experimental animals. JNPL3 mouse line was maintained as hemizygotes on an outbred Swiss Webster

background [19]. All procedures involving mice and their care were approved by the Mayo Clinic and University of Florida Institutional Animal Care and Use Committees.

Tissue extraction

Mice were euthanized by cervical dislocation in order to preserve the metabolic environment of the brain and to prevent artifacts that could alter the biochemical profiles of tau. Mouse brains were bisected down the midline to yield two hemispheres. The cerebral cortex and hippocampus (ctx+hip) of the right hemisphere of each animal were quickly frozen on dry ice and stored at −80°C until use. Tissues were then homogenized in 10 volumes of Tris-buffered saline [TBS: 50 mM Tris/HCl (pH 7.4), 274 mM NaCl, 5 mM KCl, 1% protease inhibitor mixture (Sigma, St. Louis, MO), 1% phosphatase inhibitor cocktail I & II (Sigma), and 1 mM phenylmethylsulfonyl fluoride (PMSF)] [14,15]. The homogenates were either centrifuged at 150,000 × g (protocol A) or 27,000 × g (protocol B) for 20 min at 4°C to obtain supernatant (S1) and pellet fractions (Figs. 1A, B). Pellets were homogenized in 5 volumes of high salt/sucrose buffer [0.8 M NaCl, 10% sucrose, 10 mM Tris/HCl, (pH 7.4), 1 mM EGTA, 1 mM PMSF] and centrifuged as above. The supernatants were collected and incubated with sarkosyl (1% final concentration; Sigma) for one hour at 37°C, followed by centrifugation at 150,000 × g for one hour at 4°C to obtain salt and sarkosyl-extractable (S3) and sarkosyl-insoluble (P3) fractions. The P3 pellet was re-suspended in TE buffer [10 mM Tris/HCl (pH 8.0), 1 mM EDTA] to a volume equivalent to half of that of the brain specimens used to produce brain homogenates. To prepare heat-stable samples, we incubated a portion of the S1 fraction at 95°C for 10 min followed by centrifugation at 27,000 × g for 20 min. The supernatants were concentrated by using a centrifugal filter (Amicon Ultra, Millipore, MA) and subjected to SDS-PAGE. The separated protein bands were visualized through CBB staining using a SimpleBlue™ SafeStain kit (Invitrogen, Grand Island, NY). Human temporal cortices were provided by the Mayo Clinic Jacksonville brain bank for neurodegenerative disorders. Tissue extraction was followed by protocol B as shown above. The experimental procedure involving human tissues was approved by the Mayo Clinic institutional review board.

Western blotting and dot blotting

Fractionated tissue extracts were dissolved in SDS-sample buffer containing β-mercaptoethanol (2.5%). The heat-treated samples (60°C for 15 min) were separated by gel electrophoresis on 10% Tris-glycine SDS-PAGE gels or 4–12% Bis-Tris SDS-PAGE gels containing a 15-well comb (Invitrogen) and transferred onto nitrocellulose membranes (BioRad Laboratories, Hercules, CA). For dot blotting, samples were pre-treated by Dynabeads Protein G (Invitrogen) to absorb mouse IgG background. 20 μl of Dynabeads were washed with PBS and mixed with 200 μl of S1 fraction. The mixture was incubated on a rotator overnight at 4°C. 1 μl of each immune-depressed sample was spotted on nitrocellulose membranes. After blocking with a blocking solution containing 5% nonfat milk and 0.1% Triton-X100 in TBS, the membranes were incubated with various antibodies, washed to remove excess antibodies, and then incubated with peroxidase-conjugated goat anti-rabbit antibodies (1:5000; Jackson ImmunoResearch, West Grove, PA) or anti-mouse IgG (1:5000; Jackson ImmunoResearch). Bound antibodies were detected using an enhanced chemiluminescence system (ECL PLUS kit; PerkinElmer). Western blot immunoreactivity was visualized by a computer-linked LAS-4000 BioImaging Analyzer System (Fujifilm, Tokyo, Japan) and quantitative analysis was performed by Multi Gauge v3.1 software (Fujifilm). To detect tau protein, we subjected different fractions (S1, S3, P1) derived from 0.01 mg of tissue to SDS-PAGE. For comparing different fractions, we loaded S1, S3, and P3 fractions into gels at a ratio of 1:16:50 (based on tissue weight). To quantitate tau protein and to compare tau protein levels across individual mouse brains, we determined the relative amounts of tau in S1 by normalizing tau protein levels by those of glyceraldehyde-3-

phosphate-dehydrogenase (GAPDH). For the inter-gel standard, three mouse brain samples were selected and loaded into each gel. Then, the averaged relative amount of these samples was used for the correction between multiple blot intensities.

Antibodies

We used polyclonal tau antibodies E1, WKS44, and WKS46 [20]; pS212 (Invitrogen); and pS422 (Invitrogen); and monoclonal tau antibodies PHF1, CP13, and MC1 (provided by Dr. Peter Davies, Albert Einstein College of Medicine); Ab39 [21,22]; Tau5 (provided by Dr. Lester I. Binder, Northwestern University Medical School); Tau13 (Covance, Emeryville, CA); 12E8 (provided by Dr. Peter Seubert, Elan Pharmaceuticals); PHF6 (AbCam); and Tau46 (Zymed). Of the aforementioned antibodies, PHF1, PHF6, CP13, 12E8, pS212, and pS422 recognize phosphorylated epitopes. The remaining antibodies recognize non-phosphorylated epitopes. The location of epitopes recognized by different antibodies is listed in Supplemental Table 1. Other monoclonal antibodies used were specific to GAPDH (Biodesign, Saco, ME); β-actin; or β-tubulin (Sigma).

Two-dimensional SDS-polyacrylamide gel electrophoresis (2D SDS-PAGE)

S1 fraction samples were prepared in rehydration solution containing 7 M urea, 2 M thiourea, and IPG buffer using 2-D Clean-Up Kit (GE Healthcare Life Science, Piscataway, NJ). They were loaded onto 11 cm IPG strips (pH 4–7 or pH 3–10; GE Healthcare Life Science), followed by isoelectric focusing. Second dimension separation was performed with 10% SDS-PAGE at 150 V using the Criterion™ gel electrophoresis system (BioRad Laboratories). Subsequently, gels were transferred onto nitrocellulose membranes (BioRad Laboratories) for Western blotting using tau antibodies WKS44 and PHF1.

Immunogold electronmicroscopy

Samples were adsorbed onto carbon/formvar-coated 400 mesh copper grids (EM Science, Fort Washington, PA) for 60 sec. After washing with filtered TBS three times, the grids were blocked for 15 min in blocking solution (filtered TBS containing 0.04% bovine serum albumin and 2% horse serum), and then incubated for 2 hours with Tau46 (1:50) and E1 (1:20) antibodies. Excess antibodies were removed by washing with the blocking solution three times. The grids were subsequently incubated for 1 hour in 5 nm gold-conjugated anti-rabbit and 10 nm gold-conjugated anti-mouse secondary antibodies (1:20; GE Healthcare Life Science). After washing with TBS five times, the grids were stained with 2% uranyl acetate for 45 sec and examined with a Philips 208S electron microscope (Philips, Hillsboro, OR). All antibodies were diluted with the blocking solution.

Statistical analysis

Statistical analysis was conducted using PRISM4 (GraphPad Software Inc., La Jolla, CA) and one-way ANOVA, unless noted otherwise.

RESULTS

Isolation of TBS-extractable 64 kDa tau

In previous studies of rTg4510 mice [14,23], brain homogenates were centrifuged at 150,000 × g (protocol A) to yield supernatant and pellet fractions (Fig. 1A). The pellet was subsequently treated with high salt/sucrose buffer and centrifuged as above. The supernatants were treated with sarkosyl and separated into sarkosyl-extractable and sarkosyl-insoluble fractions. In the present study, we followed a different protocol (protocol B), in which tissue homogenates were centrifuged at 27,000 × g. This protocol has previously been used to study abnormal tau from AD brains (Fig. 1A) [24]. Regardless of

the protocols, supernatant fractions obtained from the first centrifugation step (S1 fraction) of brain and spinal cord preparations from aged rTg4510 tau transgenic mice contain tau proteins of size [50–60 kDa; consistent with that of normal tau (Fig. 1B)], as determined by immunoblotting. Larger sized tau of 64 kDa in molecular weight, referred to as TBS-extractable 64 kDa, was recovered only in the S1 fraction following protocol B in aged rTg4510 transgenic mice (Fig. 1B). Such tau species, detected in brain specimen from rTg4510 mice were not found in spinal cord – a region that displayed no tauopathy (Fig. 1B) [14]. TBS-extractable 64 kDa tau was also demonstrated in the S1 fraction from the aged constitutive transgenic model, JNPL3, in which the same 0N4R human P301L tau is overexpressed as in rTg4510 mice, but at lower levels and in an altered expression pattern [5]. We analyzed brain and spinal cord extracts derived from a female 16 month-old JNPL3 mouse which displayed hind limb paralysis, a phenotype that we have previously shown correlates with degree of tauopathy in the spinal cord of this model [19]. Similar to brain extracts from rTg4510 mice, brain extracts from JNPL3 mice also contained the TBS-extractable 64 kDa tau, though at a lesser extent. The preponderance of this TBS-extractable 64 kDa tau in JNPL3 mice was observed in the spinal cord, which is a main site of tauopathy in this model (Fig. 1B and C).

To further confirm the existence of TBS-extractable 64 kDa tau in S1 fraction recovered by low speed centrifugation (27,000 × g, protocol B in Fig. 1A and B), we analyzed rTg4510 mice ranging from 2 month to 14 months, time points that cover the progression from early to severe tauopathy in this model. 64 kDa tau was detected in the S1 fraction from rTg4510 brain samples from 4 months of age onward and in the P3 fraction at all ages examined by probing with antibodies specific to hTau (E1) and phospho-tau (PHF1) (Fig. 1C). The amount of sarkosyl-insoluble tau was more abundant in 8 than 4 or 2 month-old rTg4510 mice (Fig. 1C). 64 kDa tau was rarely detected in sarkosyl-soluble (S3) fraction from rTg4510 mouse brains with E1 and PHF-1 antibodies. Similar to what was observed in rTg4510 mice, the S1 and P3 fractions from brain and spinal cords of aged JNPL3 mice with hind-limb paralysis contained 64 kDa tau immunoreactive with E1 and PHF1 antibodies. In contrast to rTg4510, the S3 fraction from JNPL3 specimens (particularly those derived from the spinal cord of mice with a more severe motor phenotype) contained appreciable levels of 64 kDa tau (Fig. 1C) that was both immunopositive for E1 and PHF1. It has been noted that P3 fraction contains filamentous tau aggregates among other elements and that enrichment of tau filaments as precipitates can be achieved via further centrifugation (150, 000 × g for 1 hour) through a sucrose density gradient [18,25]. Therefore, it is possible that 64 kDa tau in S1 and S3 fractions were constituents of tau assemblies at earlier stages of tau-self interactions.

Distinct property of TBS-extractable 64 kDa tau

To determine the relative amounts of hTau in different fractionations derived from rTg4510 mice, we performed quantitative analysis of E1 antibody immunoblotting of samples from 3 to 4 and 6 to 8 month-old animals according to protocol B. Upon correction for differences in sample dilution, we determined the proportion of total human tau (i.e. S1+S3+P3) in different fractions. As summarized in Fig. 1D, more than 93% of tau was recovered in the S1 fraction, followed by S3 and P3 fractions, which represent less than 6.3% and 0.5% of the total, respectively. The proportion of tau in P3 fractions increased with age of animals (6–8 versus 3–4 month-old). Of those partitioned into S1 fraction of the brain, only ~3% was due to the presence of 64 kDa tau species in rTg4510 mice between 3 and 4 months of age, though this increased to ~14% in 6 to 8 month-old rTg4510 mice. Our quantitative analysis also showed the presence of about 78–80 times more 64 kDa tau in the S1 than in the P3 fraction (Fig. 1D).

We next carried out detailed analyses of tau in 1 to 14 month-old rTg4510 mice, focusing on the S1 and P3 fractions, since the S3 fraction did not contain abnormal sized tau. To analyze the progression of tau phosphorylation, blotting was performed with PHF1 antibody (Fig. 2A), which was widely used for the detection of hyperphosphorylated tau [26,27]. In addition to the aforementioned 64 kDa tau species, larger sized tau species were present in samples from 4 months and older mice and more abundant in older ones (Fig. 2A). In the S1 fraction, most large tau species were discerned as discrete bands upon immunoblotting. In contrast, most large tau in the P3 fraction appeared as smears displaying wide ranges of electrophoretic mobility (Fig. 2A; bottom panel). A portion of high molecular weight (HMW) tau in the P3 fraction from rTg4510 brain (indicated arrows in Fig. 2A) was too large to enter the gel, and the amount of HMW tau in the P3 increased with age and severity of tauopathy in rTg4510 mice. The results raise the possibility that 64 kDa tau species partitioned to the S1 fraction were at earlier states of self-assembly and/or less modified than those located in the P3 fraction. Upon quantitative analysis of 64 kDa tau in the S1 fraction versus brain weight, we demonstrated a significant inverse correlation between these two parameters (Fig. 2B, D), regardless whether animals of all ages, 1 to 8 month-old or 14 month-old were considered. In this regard, it has been reported that tauopathy causes progressive, age-dependent forebrain atrophy in rTg4510 mice [14,28]. Similar analysis showed a significant inverse relationship between the levels of 64 kDa in the P3 fraction and brain weight, when mice of all ages or 8 month-old or younger were examined (Fig. 2C, D). However, for 1 to 6 month-old mice the relationship between sarkosyl-insoluble 64 kDa tau and brain weight is not as well correlated as that displayed by the TBS-extractable tau and brain weight (i.e. $p=0.1003$ versus $p=0.0018$) (Fig. 2D). In addition, dot blot analysis of the P3 fraction showed an age-dependent increase of PHF1-immunoreactivity until 6 months of age. However, the inverse correlation between the total amount of sarkosyl-insoluble tau and brain weight disappeared in mice over 6 months of age (data not shown). These results suggest that the level of TBS-extractable 64 kDa tau species appears to reflect neuronal loss better than that of sarkosyl-insoluble tau species.

Phosphorylation sites in TBS-extractable 64 kDa tau

To analyze tau phosphorylation, we probed blots of S1 fractions derived from brain extracts from 4 and 8 month-old rTg4510 mice with a panel of tau antibodies against phosphorylation-dependent or phosphorylation-independent tau epitopes (Fig. 3A). TBS-extractable 64 kDa tau (indicated by arrows on right side of blots in Fig. 3A) was readily detected by nine phosphorylation-dependent antibodies tested (AT270, CP13, pS212, AT100, PHF6, 12E8, PHF1, pS400, and pS422). By contrast, some of these phosphorylated epitopes were hardly detected in normal tau (indicated by bold lines on right side of blots in Fig. 3A), even though the level of normal tau is much higher than that of 64 kDa tau according to immunolabeling with phosphorylation-independent tau antibodies (E1, WKS44, and Tau46). The results support the notion that TBS-extractable 64 kDa tau differs from normal tau in the extent of phosphorylation and is phosphorylated at multiple sites.

To evaluate tau phosphorylation during the progression of tauopathy in this model, we probed Western blots of S1 fraction with 12E8, PHF1 and E1 antibodies and performed quantitative analysis (Fig. 3B). The ratios of phosphorylated tau to total tau (50–64 kDa) (e.g., 12E8 versus E1, respectively) were determined and values derived from samples of 2 month-old mice were regarded as one. As summarized in Fig. 3C, the proportion of phosphorylated tau increased as the age of mice increased. The extent of tau phosphorylation in 8 month-old mice is as high as sevenfold (Fig. 3C) of that from 2 month-old.

Besides immunoblotting with phosphorylation-dependent antibodies, we used 2D SDS-PAGE at pH 3–10 and pH 4–7 to profile tau phosphorylation in the S1 fraction of rTg4510

mouse brain at 6 months. After 2D electrophoresis was completed, proteins in polyacrylamide gel were transferred to nitrocellulose membrane and blotted by phosphorylation-independent tau antibody WKS44. As a result, 2D SDS-PAGE/Western blot (2D-Western blot) analysis of S1 fraction from 6 month-old rTg4510 mice revealed multiple 64 kDa tau isoforms having isoelectric points ranging from pH 5.0 to pH 6.0 (validated by control proteins β-tubulin and β-actin as shown in Fig. 3E), values that are far more acidic than the theoretical isoelectric point (pH 9.4) of the 4R0N tau isoform, which contains the P301L mutation (Fig. 3D & E). 2D-Western blot by using PHF1 antibody confirmed that hyperphosphorylated 64 kDa tau was displayed to multiple spots (Fig. 3D). These data support further that 64 kDa tau is modified by phosphorylation. Interestingly, it should be noted that multiple spots of 64 kDa tau were migrated to the same position on the second dimension of electrophoresis (shown in Fig. 3E) indicating that the mobility shift of the 64 kDa tau was not entirely dependent on increased molecular weight by additional phosphorylation.

Distinction between normal and TBS-extractable 64 kDa tau in sedimentations properties and reaction to reducing agent

To find out whether normal and TBS-extractable 64 kDa tau have different physicochemical properties, the S1 fraction from 6 month-old rTg4510 mice was centrifuged further at 150,000×g for 20 min to obtain a supernatant (S1c) and a pellet (S1p) fraction (Fig. 4A). When the S1p fraction was analyzed under reducing (+β-mercaptoethanol [βME], Fig. 4B) and non-reducing conditions, most of the tau was detected in the region around 64 kDa (arrow in Fig. 4A) and ~ 130 kDa (dimer in Fig. 4B), respectively. In comparison, the electrophoretic mobility of most tau in S1c is comparable to normal tau and was not affected by the presence or absence of reducing agent βME (Fig. 4B). The results indicate the presence of tau assemblies in S1p preparation and the involvement of disulfide bond cross-linkage in tau-self interaction, and are consistent with previous findings of cysteine-dependent tau dimers [29,30].

To test whether TBS-extractable 64 kDa tau is comparable to normal tau in terms of thermo-stability, the S1c and S1p fractions were heat-treated at 95°C for 10 min, and centrifuged to separate heat-stable from heat-unstable proteins. Similar preparations from non-transgenic mice were used as controls and 4R0N recombinant tau was included as a reference. All heat-treated samples were separated by SDS-PAGE, stained with Coomassie blue or probed with E1 and PHF1 antibodies by Western blotting (Supplemental Fig. 1). Coomassie blue staining showed the presence far more 50–60 kDa (marked by bracket) and 64 kDa (marked by arrow) proteins in rTg4510 than non-transgenic preparations, when samples from S1c and S1p fractions, respectively, were analyzed (Supplemental Fig. 1). Importantly, these sized proteins displayed E1 and PHF1 immunoreactivities, indicating that TBS-extractable 64 kDa tau is as thermo-stable as normal tau (Supplemental Fig. 1).

Ultrastructural analysis of TBS-extractable 64 kDa tau

To determine the morphological properties of tau assemblies located in the S1p fraction, we used electron microscopy with or without immunogold labeling. Numerous granular aggregates and short filaments (~200 nm in length and 10–17 nm in width) were detected in S1p samples derived from 6-month-old rTg4510 mice (Fig. 4, C and E). Structures were rarely detected in corresponding preparation from 6 month-old non-transgenic controls (Fig. 4D). By counting the number of granules and filaments in multiple fields (9 fields, 1.8 μm × 1.8 μm), we estimated that granular elements represent about 30% of the total (n=5.4±1.1 in an area of 3.24 μm^2) and the rest were short filaments (n=13.9±1.1 in an area of 3.24 μm^2).

Immunogold labeling of S1p samples revealed tau immunoreactivities in granular and short filamentous structures (Fig. 4, G and H). Since the P3 fraction contained 64 kDa tau species and has previously been shown to contain filamentous elements, we determined whether there are dimensional differences between such filaments and those recovered in the S1p fraction. Conventional transmission electron microscopic analysis of samples revealed the presence of filaments that were much longer in the P3 than those in S1p fraction (Fig. 4, E and F). The results as well as those obtained from biochemical profiling of tau are consistent with the notion that the S1p fraction contains tau at earlier stages of assembly than P3.

Relevance of TBS-extractable 64 kDa tau to tauopathy in FTDP-17

To determine the relevance of TBS-extractable 64 kDa tau to human tauopathy, we fractionated human brain homogenates from FTDP-17 harboring P301L mutation, using protocol B and centrifugation of the S1 fraction at 150,000×g to derive S1c and S1p fractions. Because the level of hTau in rTg4510 mouse brain is significantly higher than that in human brain, we loaded 20-fold more FTDP-17 human brain sample so that the Western blots would show comparable intensities. As the sample loading ratio of human brain samples was different from the rTg4510 mouse brain samples, the intensity of S3 fractions from human brain samples was much less than that from rTg4510 mouse brain samples (Supplemental Fig. 2). Similar to what was observed in rTg4510 mice, S1p and P3 fractions from human specimens contained higher molecular weight, phosphorylated tau species (e.g. 12E8 and PHF1 immunoreactive) larger than normal tau (Supplemental Fig. 2 and Fig. 4A) - some did not enter the gel and others appeared as smears. The electrophoretic profiles of tau in samples derived from human FTDP-17 brain are more complex than those in corresponding preparations from rTg4510 mice. In the P3 fraction, three distinctive tau species of size 60, 64 and 68 kDa were detected in samples from human as previously reported [18,31], but only 64 kDa tau was found in those from transgenic mice. The difference between human FTDP-17 and rTg4510 samples likely reflects the presence of multiple human tau isoforms in human brain rather than the single 0N4R human tau isoform found in the rTg4510 model. The human FTDP-17 samples contained a number of lower molecular weight products which were absent in the rTg4510 samples, and this may reflect degradation that is associated with post-mortem delay associated with human studies.

Pathological alteration of TBS-extractable 64 kDa tau

To confirm early pathological alteration of 64 kDa tau species, both S1c and S1p fractions were examined for the immunoreactivity of MC1, Ab39 and Tau13 antibodies (Fig. 5). The MC1 antibody recognized specific tau conformation in which the amino-terminal region comes into contact with the microtubule-binding domains [32]. The conformational change from normal unfolded state to this compact folding state has been considered to be essential for tau aggregation process [27,33]. The Ab39 antibody is known to recognize a unique epitope in NFT although its precise epitope is still unknown due to difficulties associated with its use for Western blotting analysis [22,34]. Tau13 antibody is hTau specific and phosphorylation-independent monoclonal antibody. Our dot blotting data clearly showed that MC1-immunoreactivity in S1p fraction from rTg4510 mice was significantly higher than that in S1p fraction from non-tg mice at both 2.5 and 8 months of age (Fig. 5B). Based on pathological alteration of tau in rTg4510 mice, it was reasonable that the P3 fraction from 8 month-old rTg4510 mice showed higher MC1-immunoreactivity than the P3 fraction from 2.5 month-old rTg4510 mice (Fig. 5B). On the other hand, Ab39-immunoreactivities in both S1c and S1p fractions from rTg4510 mice were not significantly different from those from non-tg mice (Fig. 5C) while Tau13-immunoreactivities in those fractions from rTg4510 were clearly positive to compare with those from non-tg mice (Fig. 5D). As the Ab39 antibody preferentially detects NFT in tauopathy brains [19,22,34], Ab39-immunoreactivity was only positive in P3 fraction from 8 month-old rTg4510 mice (Fig. 5C). Similar to the

MC1 antibody, Tau13-immunoreactivity in P3 fraction from 8 month-old rTg4510 mice was higher than that in P3 fraction from 2.5 month-old rTg4510 mice (Fig. 5D). These data suggest that TBS-extractable 64 kDa tau has a MC1-positive conformation, and differs from mature tangles.

DISCUSSION

Findings of tau mutations in frontotemporal dementia affected subjects and mutant tau expression causing formation of tau-positive inclusions, neuronal loss and behavior abnormalities in various animal models have established a role of this protein in neurodegeneration [5–12]. The abundance of NFTs has been reported to correlate positively with the severity of cognitive impairment in AD [35]. However, accumulating evidences derived from studies of experimental models have indicated that NFTs may not be neurotoxic. For example, a *Drosophila* model of tauopathy showed neuronal cell loss without NFT formation [36] and suppression of hTau overexpression in a transgenic mouse model prevented further neuronal loss and cognitive impairment without decreasing NFT count [14]. These studies suggest that tau assemblies at certain stages of self-interactions before NFTs are formed may be involved in neuronal loss.

To identify tau species related to the development of tauopathy and progression of neuronal dysfunction, we examined tau protein biochemistry in an inducible P301L mutant htau transgenic mouse model. As demonstrated in the present study, induced hTau expression caused an age-dependent increase of TBS-extractable tau of 64 kDa in molecular weight. This form of tau is larger than normal tau, recoverable in the supernatant (S1) fraction following centrifugation of brain homogenates at 27,000 × g, and separable from normal tau after further centrifugation at 150,000 × g, and abnormally phosphorylated. In the brains of FTDP-17 patients, hyperphosphorylated tau was also recovered in the fraction recovered following 27,000 × g to 150,000 × g centrifugation. Our results are in line with previous findings showing that AD P-tau is primarily isolated from the 27,000 × g to 200,000 × g fraction of AD brain extracts [16]. Immunochemical and morphological analyses showed that less than 30% of tau in the AD P-tau fraction is derived from filamentous species [16]. Consistent with these observations, we did not find tau filaments (>200 nm length) in the TBS-extractable 64 kDa tau preparations. Instead, we observed amorphous, tau-immunopositive granular aggregates and short filaments. This morphological finding was further supported by MC1 immunoreactivity and Ab39 insensitivity. The MC1 antibody, which was raised to Alz50 [37] immunoaffinity purified paired helical filaments from AD brain [32], identifies an early pathogenic conformation of tau [27]. On the other hand, the Ab39 antibody raised to crude AD brain homogenate preferentially detects NFTs [21,22,34]. Our results indicate that the TBS-extractable 64 kDa tau-enriched fraction contains tau products with abnormal conformation at less advanced stages of self-assembly than NFTs. Interestingly, in brain samples from 6 month-old rTg4510 mice, there was ~80 times more 64 kDa tau in the TBS-extractable fraction than in the sarkosyl-insoluble fraction, indicating that more than 95% of 64 kDa tau may comprise soluble tau species. In Western blots, sarkosyl-insoluble tau from human tauopathy brains appears high molecular weight smears (see Supplemental Fig. 2 and [24,38,39]). Although these high molecular smear species can be accounted as a major pool of hyperphosphorylated tau from human diseased brain, the 64 kDa tau in the TBS-extractable fraction from rTg4510 mice was more abundant than htau immunoreactive smear in sarkosyl-insoluble fraction from rTg4510 mice (see Supplemental Fig. 2 and note that S1 and P3 fraction were derived from 0.01 and 0.5 mg of tissue, respectively). Therefore, it is possible that soluble hyperphosphorylated tau species, not NFTs, are involved in neuronal dysfunction.

Our previous work that examined the tau aggregation pathway using an *in vitro* tau self-assembly system demonstrated the existence of tau aggregation intermediates (e.g., tau dimer, tau multimer, and granular tau oligomer) [40]. Tau multimers with apparent molecular weights of ~140 kDa and ~170 kDa have been reported in previous studies of rTg4510 brains, using a Tris-glycine gel system operating at pH 6.8 [15]. The 170 kDa tau was shown to display sarkosyl-insolubility whereas the 140 kDa species was extractable in TBS and recovered in supernatant after centrifugation at 150,000×g for 15 min [15]. Tau multimers were only observed after prolonged exposure during ECL reaction indicating that these multimers are proportionally very small fractions [15]. In our hand, analysis of TBS-extractable tau fraction using two other SDS-PAGE buffer systems—a Bis-Tris gel system operating pH of 7.0 and a Tris-acetate gel system operating pH of 8.1—showed that under non-reducing conditions tau multimers migrate to ~120 kDa and ~130 kDa, molecular sizes consistent with those of tau dimer species weighing 50–60 kDa and 64 kDa, respectively ([30,40] and Fig. 4B). We found that most tau dimers were 64 kDa tau species, whereas most tau monomers were normal tau (Fig. 4B). However, these reducing agent sensitive tau dimers were not detected in previous rTg4510 studies [15]. Although we cannot resolve this discrepancy, differences between previous and present studies were tissue preparation protocols (150,000×g and 27,000×g centrifugations for TBS-extraction, respectively) and the age of mice for the reducing agent sensitivity analysis (3.5 month-old in [15], and 6 month-old rTg4510 mice in the present study, respectively). It is conceivable that tau dimers composed of either normal tau or 64 kDa tau species can be recognized by the antibody TOC1, which was raised against cross-linked tau dimer and detected tau oligomers [41]. To determine whether cognitive function and neuronal loss are triggered by the same subspecies of tau, the correlation analysis between cognitive performance of rTg4510 mice and levels of TBS-extractable 64 kDa tau species need to be examined in future.

Mass spectrometric analysis and mapping using phosphoepitope-specific antibodies of AD brain samples have revealed that insoluble tau possesses 45 phosphorylation sites (for review, see [42]). Under physiological conditions, tau phosphorylation sites may turn over rapidly through the regulation of multiple kinases and phosphatases. In brains undergoing tauopathy, abnormal highly phosphorylated tau seems to influence self-aggregation by maintaining a stable state of phosphorylation. In the present study, we observed more than 10 phosphoepitope-positive sites on TBS-extractable 64 kDa tau in 8 month-old rTg4510 mice. Two-dimensional gel electrophoresis revealed that 64 kDa tau has multiple isoelectric points, ranging from pH 5.0 to pH 6.0. By contrast, the 4R0N tau isoform with P301L mutation has a theoretical isoelectric point of pH 9.4. Taken together, this indicates that the phosphorylation sites in 64 kDa tau neutralize the basic charge of tau. Most interestingly, multiple isoelectric points of 64 kDa tau indicate that 64 kDa tau is heterogeneously phosphorylated. Since it remains unknown which specific phosphorylation sites underlie the mobility shift of tau proteins in SDS-PAGE, it would be worthwhile to perform phosphopeptide mass spectrometry of TBS-extractable 64 kDa tau species.

In summary, the progression of tauopathy in rTg4510 mice is closely associated with the levels of a pool of abnormal tau. This abnormal tau appears as short filaments and granules representing oligomeric assemblies of 64 kDa hyperphosphorylated tau. Oligomer formation involves disulfide cross-linking between tau molecules. The resulting assembly intermediates are much more abundant than the end products of assembly. Our research goal is to identify the tau species that must be eliminated in order to halt or reverse tau-induced neurodegeneration. If the TBS-extractable 64 kDa tau species can be reversibly regulated, our finding will provide crucial information toward development of tau-based therapy.

Supplementary Material

Refer to Web version on PubMed Central for supplementary material.

Acknowledgments

The authors thank Dr. L.I. Binder (Northwestern University Medical School, Chicago, IL) for providing the monoclonal anti-tau antibodies Tau1 and Tau5, Dr. P. Davies (Albert Einstein University, Bronx, NY) for the monoclonal anti-tau antibodies, CP13, and PHF-1, and Dr. P. Seubert (Elan Pharma, South San Francisco, CA) for the monoclonal anti-tau antibody 12E8. This research was supported in part by grants from the Thomas H. Maren Junior Investigator Fund (N.S.), National Institutes of Health/National Institute of Neurological Diseases and Stroke R21 NS067127 (N.S.), 5R01NS046355 (J.L.), the Alzheimer's Association IIRG-06-27277-1 (J.L.), H. Lundbeck A/S (C.V., J.T.P., J.L.) and Mayo Foundation (J.L.).

References

1. Lee VM, Goedert M, Trojanowski JQ. Neurodegenerative tauopathies. Annu Rev Neurosci. 2001; 24:1121–1159. [PubMed: 11520930]
2. Swaab DF, Dubelaar EJ, Hofman MA, Scherder EJ, van Someren EJ, Verwer RW. Brain aging and Alzheimer's disease; use it or lose it. Prog Brain Res. 2002; 138:343–373. [PubMed: 12432778]
3. Binder LI, Guillozet-Bongaarts AL, Garcia-Sierra F, Berry RW. Tau, tangles, and Alzheimer's disease. Biochim Biophys Acta. 2005; 1739:216–223. [PubMed: 15615640]
4. Gomez-Isla T, Hollister R, West H, Mui S, Growdon JH, Petersen RC, Parisi JE, Hyman BT. Neuronal loss correlates with but exceeds neurofibrillary tangles in Alzheimer's disease. Ann Neurol. 1997; 41:17–24. [PubMed: 9005861]
5. Lewis J, McGowan E, Rockwood J, Melrose H, Nacharaju P, Van Slegtenhorst M, Gwinn-Hardy K, Paul Murphy M, Baker M, Yu X, Duff K, Hardy J, Corral A, Lin WL, Yen SH, Dickson DW, Davies P, Hutton M. Neurofibrillary tangles, amyotrophy and progressive motor disturbance in mice expressing mutant (P301L) tau protein. Nat Genet. 2000; 25:402–405. [PubMed: 10932182]
6. Gotz J, Chen F, Barmettler R, Nitsch RM. Tau filament formation in transgenic mice expressing P301L tau. J Biol Chem. 2001; 276:529–534. [PubMed: 11013246]
7. Tanemura K, Akagi T, Murayama M, Kikuchi N, Murayama O, Hashikawa T, Yoshiike Y, Park JM, Matsuda K, Nakao S, Sun X, Sato S, Yamaguchi H, Takashima A. Formation of filamentous tau aggregations in transgenic mice expressing V337M human tau. Neurobiol Dis. 2001; 8:1036–1045. [PubMed: 11741399]
8. Tatebayashi Y, Miyasaka T, Chui DH, Akagi T, Mishima K, Iwasaki K, Fujiwara M, Tanemura K, Murayama M, Ishiguro K, Planel E, Sato S, Hashikawa T, Takashima A. Tau filament formation and associative memory deficit in aged mice expressing mutant (R406W) human tau. Proc Natl Acad Sci U S A. 2002; 99:13896–13901. [PubMed: 12368474]
9. Allen B, Ingram E, Takao M, Smith MJ, Jakes R, Virdee K, Yoshida H, Holzer M, Craxton M, Emson PC, Atzori C, Migheli A, Crowther RA, Ghetti B, Spillantini MG, Goedert M. Abundant tau filaments and nonapoptotic neurodegeneration in transgenic mice expressing human P301S tau protein. J Neurosci. 2002; 22:9340–9351. [PubMed: 12417659]
10. Schindowski K, Bretteville A, Leroy K, Begard S, Brion JP, Hamdane M, Buee L. Alzheimer's disease-like tau neuropathology leads to memory deficits and loss of functional synapses in a novel mutated tau transgenic mouse without any motor deficits. Am J Pathol. 2006; 169:599–616. [PubMed: 16877359]
11. Yoshiyama Y, Higuchi M, Zhang B, Huang SM, Iwata N, Saido TC, Maeda J, Suhara T, Trojanowski JQ, Lee VM. Synapse loss and microglial activation precede tangles in a P301S tauopathy mouse model. Neuron. 2007; 53:337–351. [PubMed: 17270732]
12. Eckermann K, Mocanu MM, Khlistunova I, Biernat J, Nissen A, Hofmann A, Schonig K, Bujard H, Haemisch A, Mandelkow E, Zhou L, Rune G, Mandelkow EM. The beta-propensity of Tau determines aggregation and synaptic loss in inducible mouse models of tauopathy. J Biol Chem. 2007; 282:31755–31765. [PubMed: 17716969]

13. Mayford M, Bach ME, Huang YY, Wang L, Hawkins RD, Kandel ER. Control of memory formation through regulated expression of a CaMKII transgene. Science (New York, NY. 1996; 274:1678–1683.
14. Santacruz K, Lewis J, Spires T, Paulson J, Kotilinek L, Ingelsson M, Guimaraes A, DeTure M, Ramsden M, McGowan E, Forster C, Yue M, Orne J, Janus C, Mariash A, Kuskowski M, Hyman B, Hutton M, Ashe KH. Tau suppression in a neurodegenerative mouse model improves memory function. Science (New York, NY. 2005; 309:476–481.
15. Berger Z, Roder H, Hanna A, Carlson A, Rangachari V, Yue M, Wszolek Z, Ashe K, Knight J, Dickson D, Andorfer C, Rosenberry TL, Lewis J, Hutton M, Janus C. Accumulation of pathological tau species and memory loss in a conditional model of tauopathy. J Neurosci. 2007; 27:3650–3662. [PubMed: 17409229]
16. Kopke E, Tung YC, Shaikh S, Alonso AC, Iqbal K, Grundke-Iqbal I. Microtubule-associated protein tau. Abnormal phosphorylation of a non-paired helical filament pool in Alzheimer disease. J Biol Chem. 1993; 268:24374–24384. [PubMed: 8226987]
17. Alonso A, Zaidi T, Novak M, Grundke-Iqbal I, Iqbal K. Hyperphosphorylation induces self-assembly of tau into tangles of paired helical filaments/straight filaments. Proc Natl Acad Sci U S A. 2001; 98:6923–6928. [PubMed: 11381127]
18. Greenberg SG, Davies P. A preparation of Alzheimer paired helical filaments that displays distinct tau proteins by polyacrylamide gel electrophoresis. Proc Natl Acad Sci U S A. 1990; 87:5827–5831. [PubMed: 2116006]
19. Lewis J, McGowan E, Rockwood J, Melrose H, Nacharaju P, Van Slegtenhorst M, Gwinn-Hardy K, Paul Murphy M, Baker M, Yu X, Duff K, Hardy J, Corral A, Lin WL, Yen SH, Dickson DW, Davies P, Hutton M. Neurofibrillary tangles, amyotrophy and progressive motor disturbance in mice expressing mutant (P301L) tau protein. Nature genetics. 2000; 25:402–405. [PubMed: 10932182]
20. Kenessey A, Nacharaju P, Ko LW, Yen SH. Degradation of tau by lysosomal enzyme cathepsin D: implication for Alzheimer neurofibrillary degeneration. Journal of neurochemistry. 1997; 69:2026–2038. [PubMed: 9349548]
21. Yen SH, Crowe A, Dickson DW. Monoclonal-Antibodies to Alzheimer Neurofibrillary Tangles .1. Identification of Polypeptides. American Journal of Pathology. 1985; 120:282–291. [PubMed: 2411142]
22. Yen SH, Dickson DW, Crowe A, Butler M, Shelanski ML. Alzheimer's neurofibrillary tangles contain unique epitopes and epitopes in common with the heat-stable microtubule associated proteins tau and MAP2. Am J Pathol. 1987; 126:81–91. [PubMed: 2433949]
23. Ramsden M, Kotilinek L, Forster C, Paulson J, McGowan E, SantaCruz K, Guimaraes A, Yue M, Lewis J, Carlson G, Hutton M, Ashe KH. Age-dependent neurofibrillary tangle formation, neuron loss, and memory impairment in a mouse model of human tauopathy (P301L). Journal of Neuroscience. 2005; 25:10637–10647. [PubMed: 16291936]
24. Kimura T, Yamashita S, Fukuda T, Park JM, Murayama M, Mizoroki T, Yoshiike Y, Sahara N, Takashima A. Hyperphosphorylated tau in parahippocampal cortex impairs place learning in aged mice expressing wild-type human tau. The EMBO journal. 2007; 26:5143–5152. [PubMed: 18007595]
25. Sahara N, Lewis J, DeTure M, McGowan E, Dickson DW, Hutton M, Yen SH. Assembly of tau in transgenic animals expressing P301L tau: alteration of phosphorylation and solubility. J Neurochem. 2002; 83:1498–1508. [PubMed: 12472903]
26. Otvos L Jr, Feiner L, Lang E, Szendrei GI, Goedert M, Lee VM. Monoclonal antibody PHF-1 recognizes tau protein phosphorylated at serine residues 396 and 404. J Neurosci Res. 1994; 39:669–673. [PubMed: 7534834]
27. Weaver CL, Espinoza M, Kress Y, Davies P. Conformational change as one of the earliest alterations of tau in Alzheimer's disease. Neurobiol Aging. 2000; 21:719–727. [PubMed: 11016541]
28. Ramsden M, Kotilinek L, Forster C, Paulson J, McGowan E, SantaCruz K, Guimaraes A, Yue M, Lewis J, Carlson G, Hutton M, Ashe KH. Age-dependent neurofibrillary tangle formation, neuron loss, and memory impairment in a mouse model of human tauopathy (P301L). J Neurosci. 2005; 25:10637–10647. [PubMed: 16291936]

29. Barghorn S, Mandelkow E. Toward a unified scheme for the aggregation of tau into Alzheimer paired helical filaments. Biochemistry (Mosc). 2002; 41:14885–14896.

30. Sahara N, Maeda S, Murayama M, Suzuki T, Dohmae N, Yen SH, Takashima A. Assembly of two distinct dimers and higher-order oligomers from full-length tau. Eur J Neurosci. 2007; 25:3020–3029. [PubMed: 17561815]

31. Lee VM, Balin BJ, Otvos L Jr, Trojanowski JQ. A68: a major subunit of paired helical filaments and derivatized forms of normal Tau. Science. 1991; 251:675–678. [PubMed: 1899488]

32. Jicha GA, Bowser R, Kazam IG, Davies P. Alz-50 and MC-1, a new monoclonal antibody raised to paired helical filaments, recognize conformational epitopes on recombinant tau. J Neurosci Res. 1997; 48:128–132. [PubMed: 9130141]

33. Binder LI, Guillozet-Bongaarts AL, Garcia-Sierra F, Berry RW. Tau, tangles, and Alzheimer's disease. Biochim Biophys Acta. 2005; 1739:216–223. [PubMed: 15615640]

34. Dickson DW, Ksiezak-Reding H, Liu WK, Davies P, Crowe A, Yen SH. Immunocytochemistry of neurofibrillary tangles with antibodies to subregions of tau protein: identification of hidden and cleaved tau epitopes and a new phosphorylation site. Acta Neuropathol. 1992; 84:596–605. [PubMed: 1281953]

35. Grober E, Dickson D, Sliwinski MJ, Buschke H, Katz M, Crystal H, Lipton RB. Memory and mental status correlates of modified Braak staging. Neurobiol Aging. 1999; 20:573–579. [PubMed: 10674422]

36. Wittmann CW, Wszolek MF, Shulman JM, Salvaterra PM, Lewis J, Hutton M, Feany MB. Tauopathy in Drosophila: neurodegeneration without neurofibrillary tangles. Science (New York, NY. 2001; 293:711–714.

37. Wolozin BL, Pruchnicki A, Dickson DW, Davies P. A neuronal antigen in the brains of Alzheimer patients. Science. 1986; 232:648–650. [PubMed: 3083509]

38. Goedert M, Spillantini MG, Cairns NJ, Crowther RA. Tau proteins of Alzheimer paired helical filaments: abnormal phosphorylation of all six brain isoforms. Neuron. 1992; 8:159–168. [PubMed: 1530909]

39. Ihara Y, Abraham C, Selkoe DJ. Antibodies to paired helical filaments in Alzheimer's disease do not recognize normal brain proteins. Nature. 1983; 304:727–730. [PubMed: 6350889]

40. Sahara N, Maeda S, Takashima A. Tau oligomerization: a role for tau aggregation intermediates linked to neurodegeneration. Current Alzheimer research. 2008; 5:591–598. [PubMed: 19075586]

41. Patterson KR, Remmers C, Fu Y, Brooker S, Kanaan NM, Vana L, Ward S, Reyes JF, Philibert K, Glucksman MJ, Binder LI. Characterization of prefibrillar Tau oligomers in vitro and in Alzheimer disease. The Journal of biological chemistry. 2011; 286:23063–23076. [PubMed: 21550980]

42. Hanger DP, Anderton BH, Noble W. Tau phosphorylation: the therapeutic challenge for neurodegenerative disease. Trends in molecular medicine. 2009; 15:112–119. [PubMed: 19246243]

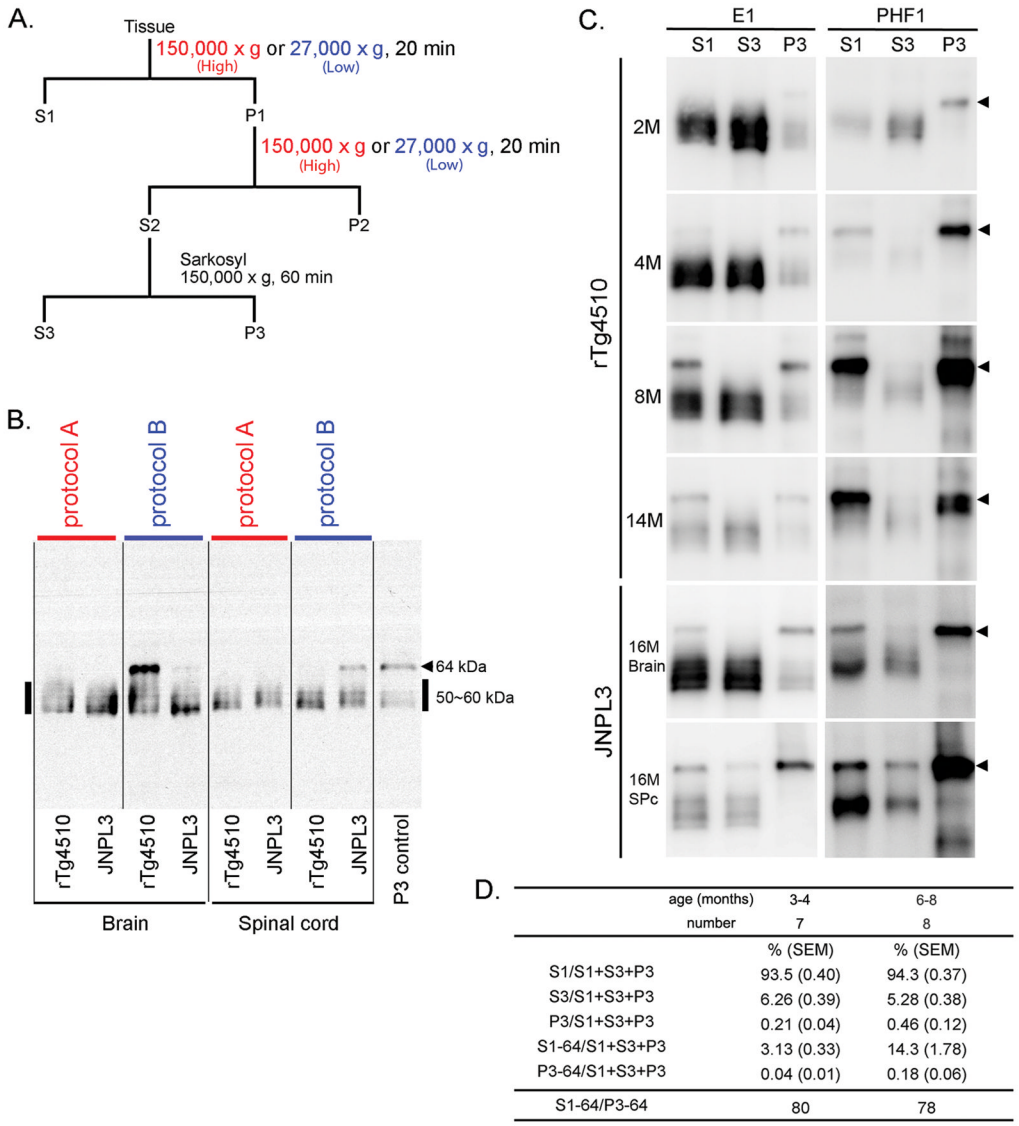

D.

	age (months)	3-4	6-8
	number	7	8
		% (SEM)	% (SEM)
S1/S1+S3+P3		93.5 (0.40)	94.3 (0.37)
S3/S1+S3+P3		6.26 (0.39)	5.28 (0.38)
P3/S1+S3+P3		0.21 (0.04)	0.46 (0.12)
S1-64/S1+S3+P3		3.13 (0.33)	14.3 (1.78)
P3-64/S1+S3+P3		0.04 (0.01)	0.18 (0.06)
S1-64/P3-64		80	78

Fig. 1. Sarkosyl-insoluble tau preparations from the brains of rTg4510 and JNPL3 mice: models of tauopathy

A. Comparison of two protocols for preparing sarkosyl-insoluble tau. Brain homogenates were separated into TBS-extractable (S1), high-salt and sarkosyl-extractable (S3), and sarkosyl-insoluble (P3) fractions. S1 fraction was separated by centrifugation at either at 27,000 × g (protocol A) or at 150,000 × g (protocol B) for 20 min at 4°C. Pellets were re-homogenized in 5 volumes of high salt/sucrose buffer and centrifuged as above. The supernatants were collected and incubated with sarkosyl for one hour at 37°C, followed by centrifugation at 150,000 × g for one hour at 4°C to obtain salt and sarkosyl-extractable fractions (S3 fraction) and sarkosyl-insoluble pellets. B. Western blots of brain and spinal cord samples from rTg4510 and JNPL3 mice. S1 fractions from rTg4510 (13 month-old, female) and JNPL3 (16 month-old, female) mice were derived from 0.01 mg and 0.02 mg of tissue, respectively. With the two different protocols, Western blots probed with E1 antibody displayed different tau profiles. The arrow head indicates 64 kDa tau and bold line indicates 50–60 kDa tau. C. Western blots of brain samples from rTg4510 and JNPL3 mice. S1, S3, and P3 fractions were loaded at a ratio of 1:16:50 (based on tissue weight). S1 fractions from

rTg4510 and JNPL3 mice were derived from 0.01 mg and 0.02 mg of tissue, respectively. Arrowheads indicated 64 kDa tau. D. The proportion of P301L hTau in different fractions. Two age groups were analyzed from Western blots using the E1 antibody. Ratios of 64 kDa tau in the S1 fraction versus 64 kDa tau in the P3 fraction are shown at the bottom of the figure.

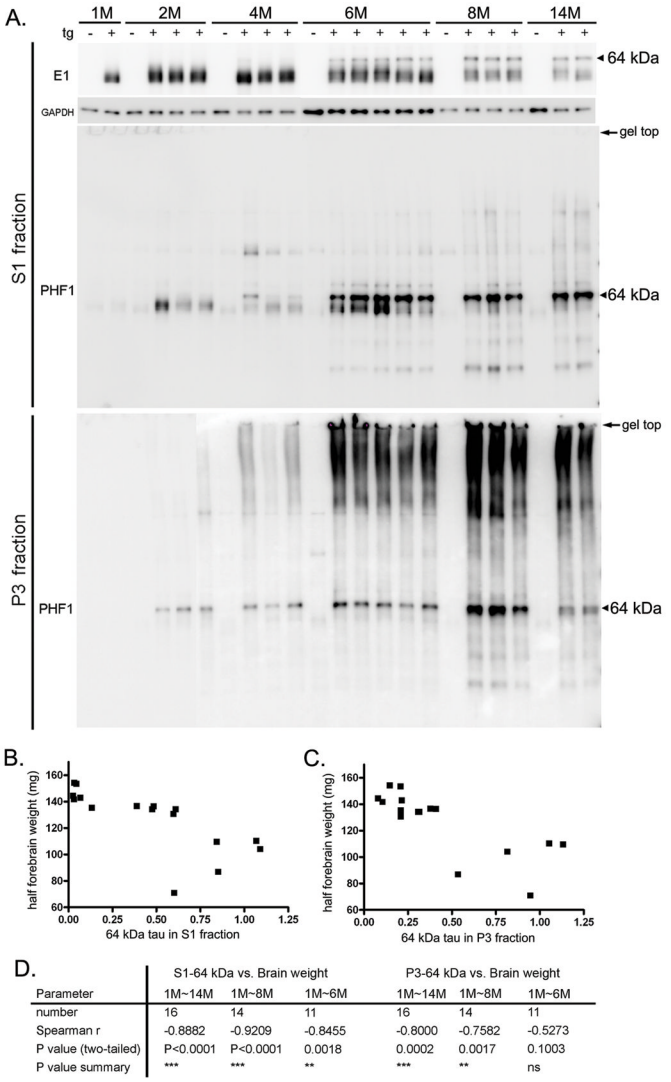

D.

Parameter	S1-64 kDa vs. Brain weight			P3-64 kDa vs. Brain weight		
	1M~14M	1M~8M	1M~6M	1M~14M	1M~8M	1M~6M
number	16	14	11	16	14	11
Spearman r	-0.8882	-0.9209	-0.8455	-0.8000	-0.7582	-0.5273
P value (two-tailed)	P<0.0001	P<0.0001	0.0018	0.0002	0.0017	0.1003
P value summary	***	***	**	***	**	ns

Fig. 2. Age-dependent 64 kDa tau accumulation and correlation with brain weight of rTg4510 mice

A. Representative Western blots showing tau (E1 and PHF1 antibodies) and GAPDH in S1 and P3 fractions derived from brains of 1, 2, 4, 6, 8 and 14 month-old rTg4510 and non-transgenic mice. The same volume of S1 and P3 fractions (containing 0.01 mg or 0.5 mg wet-weight of brain, respectively) was loaded into the gels. Arrowheads indicated 64 kDa tau. Arrows in PHF1 blots indicated positions of polyacrylamide gel top. B and C. Scatter plots showing brain weight (half of forebrain) as a function of PHF1-positive 64 kDa tau in S1 (B) and P3 (C) fractions. D. Statistical data showing the correlation between 64 kDa tau levels and brain weights. Spearman nonparametric correlation analysis was performed. Significant correlation was found: *p<0.05; **p<0.01; and ***p<0.001.

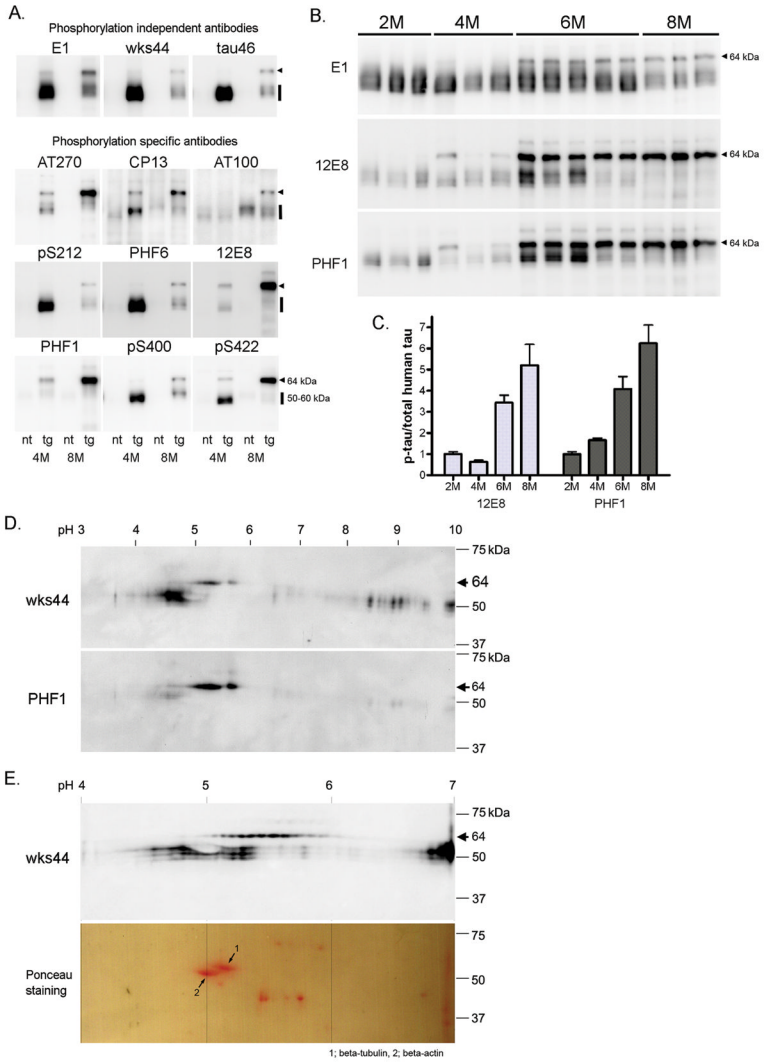

Fig. 3. Tau phosphorylation in TBS-extractable fractions from rTg4510 mouse brains

A. Western blots of TBS-extractable fractions from rTg4510 (tg) and non-tg (nt) mice aged 4 months (4 M) and 8 months (8 M) using 12 tau-specific antibodies. The same volume (containing 0.01 mg wet-weight of brain) of each sample was loaded into the gels. Arrowheads indicated 64 kDa tau. Bold lines indicated 50–60 kDa tau. B. Western blots of TBS-soluble tau derived from the brains of 2, 4, 6, and 8 month-old rTg4510 mice. Blots were probed with E1, 12E8, and PHF1 antibodies. Arrowheads indicated 64 kDa tau. C. Temporal changes in tau phosphorylation with aging. Relative phosphorylation levels detected by 12E8 and PHF1 antibodies were normalized by the levels of E1-positive tau. Values are means ± SEM with respect to levels measured from samples of 2 month-old mice; these levels were scaled to a value of one. D. Two-dimensional SDS-PAGE characterization of 64 kDa tau. Fifteen micrograms of S1 fraction from the brain of a 6 month-old rTg4510 mouse was separated via isoelectric focusing at a pH range of 4–7 (D) or 3–10 (E) for the first dimension, and then via 10% SDS-PAGE for the second dimension. The resulting blots were probed with anti-tau antibody WKS44 and anti-phosphorylated tau specific antibody PHF1. The pI of 64 kDa tau species was between 5.0 and 6.0. Arrows indicated molecular size of 64 kDa in the second dimension. Isoelectric point determination was validated using loading controls (e.g., β-tubulin, β-actin) and ponceau staining (E).

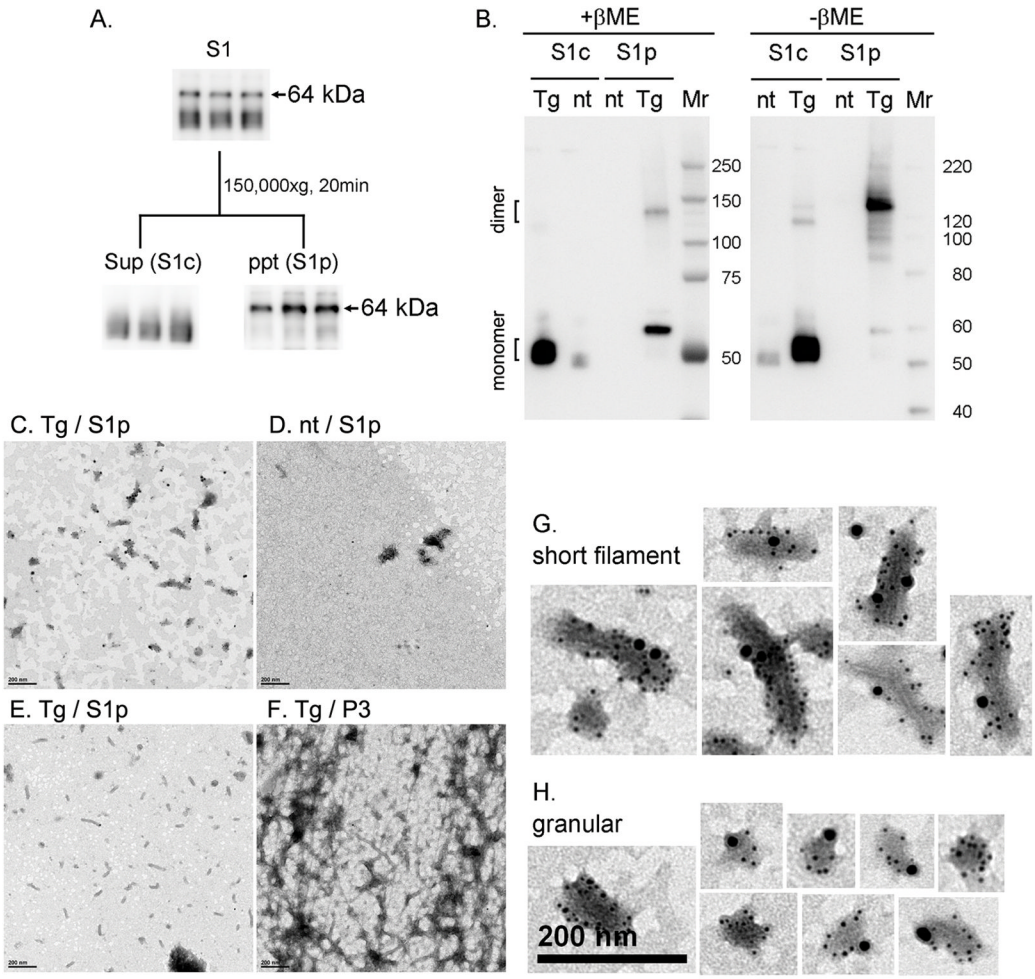

Fig. 4. Characterization of TBS-extractable 64 kDa tau

A. TBS-extractable (S1) fractions were separated by further centrifugation to 150,000 × g supernatant (S1c) and precipitate (S1p) fractions, and 64 kDa tau was recovered from the S1p fraction. B. Reducing and non-reducing SDS-PAGE and Western blotting of S1c and S1p fractions. Reducing (+βME) and non-reducing (-βME) samples were subjected to Western blotting with the Tau46 antibody. Heat-stable S1c and S1p fractions from rTg4510 (tg) and non-tg (nt) 6 month-old mice were separated by SDS-PAGE on 4–12% Bis-Tris gels using MOPS SDS running buffer. C–H. Electron microscopy analysis with or without immunogold labeling. S1p fractions from rTg4510 (C) and non-tg (D) mice were immunogold labeled with anti-E1 (4 nm gold) and anti-Tau46 (10 nm gold). Conventional transmission electron showed short filaments in S1p fraction (E) and longer filaments in P3 fraction (F). In S1p fractions from rTg4510 mice, E1 and Tau46 antibodies labeled filamentous (G) and granular (H) structures. Scale bar is 200 nm.

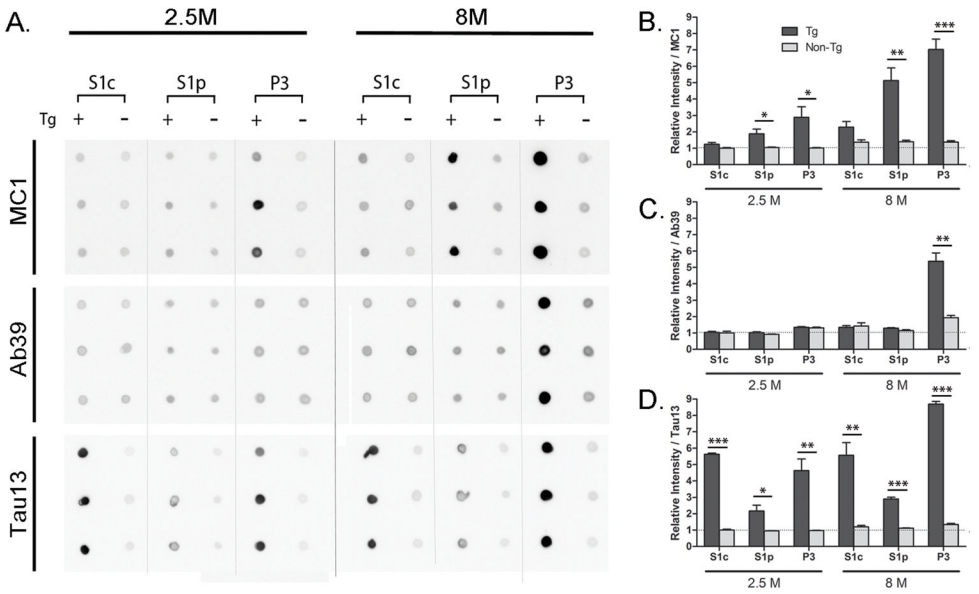

Fig. 5. Dot blot analysis of brain extracts from rTg4510 mice

A. Fractions of S1c (150,000 × g supernatant of S1) and S1p (150,000 × g precipitate of S1) and P3 fraction from rTg4510 (Tg +; n=3) and wild type control (Tg −; n=3) brain homogenates were dot blotted. Two age points were evaluated: 2.5 month-old (2.5 M) and 8 month-old (8 M). One μl of each sample was spotted on nitrocellulose membrane and probed with MC1, Ab39 and Tau13 antibodies. B. Quantification of MC1-immunopositive signals in different fraction. C. Quantification of Ab39-immunoreactive signals in different fraction. D. Quantification of Tau13-immunorective signals in different fraction. Relative signal intensities are means ± SEM normalized to the value from 2.5 month-old wild type S1c sample. Significant differences were found between rTg4510 and non-tg samples: *p<0.05; **p<0.01; and ***p<0.001.